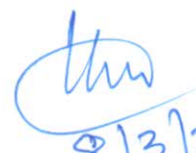


CERTIFICATE

It is certified that the work contained in the thesis titled "*Studies on Magnetic and Dielectric Properties of Mn-doped $\text{CaCu}_3\text{Ti}_4\text{O}_{12}$ synthesized through semi-wet route*" by "*Santosh Pandey*" has been carried out under my supervision and that this work has not been submitted elsewhere for a degree.

It is further certified that the student has fulfilled all the requirements of Comprehensive examination, Candidacy and SOTA for the award of Ph.D. degree.



8/3/2022

Prof. K. D. Mandal
(Supervisor)

Department of chemistry
IIT (BHU), Varanasi

DECLARATION BY THE CANDIDATE

I, "*Santosh Pandey*", certify that the work embodied in this thesis is my own bona fide work and carried out by me under the supervision of "*Prof. K. D. Mandal*" from "2017" to "2022", at the "*Department of Chemistry*", Indian Institute of Technology (Banaras Hindu University), Varanasi. The matter embodied in this thesis has not been submitted for the award of any other degree/diploma. I declare that I have faithfully acknowledged and given credits to the research workers wherever their works have been cited in my work in this thesis. I further declare that I have not will fully copied any other's work, paragraphs, text, data, results, *etc.*, reported in journals, books, magazines, reports dissertations, theses, *etc.*, or available at websites and have not included them in this thesis and have not cited as my own work.

Date: 08/03/2022

Place: varanasi

Santosh Pandey

Santosh Pandey

DECLARATION BY THE CANDIDATE

I, "*Santosh Pandey*", certify that the work embodied in this thesis is my own bona fide work and carried out by me under the supervision of "*Prof. K. D. Mandal*" from "2017" to "2022", at the "*Department of Chemistry*", Indian Institute of Technology (Banaras Hindu University), Varanasi. The matter embodied in this thesis has not been submitted for the award of any other degree/diploma. I declare that I have faithfully acknowledged and given credits to the research workers wherever their works have been cited in my work in this thesis. I further declare that I have not will fully copied any other's work, paragraphs, text, data, results, *etc.*, reported in journals, books, magazines, reports dissertations, theses, *etc.*, or available at websites and have not included them in this thesis and have not cited as my own work.

Date: 08/03/2022


Place: varanasi


Santosh Pandey

Santosh Pandey

CERTIFICATE BY THE SUPERVISOR/CO-SUPERVISOR(S)

It is certified that the above statement made by the student is correct to the best of my knowledge.


Prof. Y. C. Sharma
08032122
(Head of department)


8-3-2022
Prof. K. D. Mandal
(Supervisor)

विभागाध्यक्ष / HEAD
रसायन विज्ञान विभाग
Department of Chemistry
भारतीय प्रौद्योगिकी संस्थान (का.हि.वि.वि.)
Indian Institute of Technology (B.H.U.)
वाराणसी-221005 / Varanasi-221005

COPYRIGHT TRANSFER CERTIFICATE

Title of the Thesis: *Studies on Magnetic and Dielectric Properties of Mn-doped $\text{CaCu}_3\text{Ti}_4\text{O}_{12}$ synthesized through semi-wet route*"

Name of the Student: Santosh Pandey

Copyright Transfer

The undersigned hereby assigns to the Indian Institute of Technology (Banaras Hindu University) Varanasi all rights under copyright that may exist in and for the above thesis submitted for the award of the "Doctor of Philosophy".

Date: 08/03/2022

Place: Varanasi

Santosh Pandey
Santosh Pandey
08/03/2022

Note: However, the author may reproduce or authorize others to reproduce material extracted verbatim from the thesis or derivative of the thesis for author's personal use provided that the source and the Institute's copyright notice are indicated.



*Dedicated
To
My Beloved
family*

It's my great pleasure to thank my *supervisor Prof. K. D. Mandal*, Department of Chemistry, Indian Institute of Technology, (B.H.U) for allowing me to join his research group, and for providing the knowledge base for my future. *Prof. Mandal* is an excellent advisor and good friend. He was always available for discussions and regularly took the time to answer my many questions. As a supervisor, he was very active in my continuing education and scientific growth, allowing me to explore different aspects of materials science independently and with guidance. In addition, he continually provided opportunities for collaborations with other scientists, which allowed me to learn more about related fields.

My sincere gratitude is also expressed to **Prof. Y.C. Sharma**, Head, Department of Chemistry, Indian Institute of Technology, (B.H.U) Varanasi, for his fruitful suggestions and providing research facilities available in the Department.

It's my great pleasure to thanks my RPEC members **Prof. D.Tiwary**, Department of Chemistry, Indian Institute of Technology, (B.H.U) and **Prof. V. L. Yadav**, Department of chemical engineering, Indian Institute of Technology, (B.H.U) for helping me and giving valuable suggestions throughout my Ph.D program.

I also want to acknowledge the members of central instrumentation facility center (CIFC) and office staff of the chemistry department for their help and support.

I would also like to thank to my lab mates Vinod Kumar and Manish Kumar Verma, shruti singh, Vishnu shankar rai and Dinesh parajapati for their active support.

I am very much thankful and grateful to all faculty members of the Department for their encouragement and support.

I take great pleasure in thanking my friend Manish kr. Tirpathi, Suresh kumar Pandey, Himanshu kr.singh. Department of Chemistry BHU for sharing with me all the happiness and difficulties throughout my research work.

Parents are the God on earth and I am very lucky to have very caring and loving parents Mr. Swaminath Pandey, and Mrs. Kesh kumari I would like to put in words my gratitude to my family members for making my life happy with their constant love.

ACKNOWLEDGMENTS

I wish to express my special thanks to the funding agency, IIT(BHU) for providing the financial support to carry out this work.

Last but not least, I thank almighty God for providing me strength and courage to do this work.

Date:

Place: Varanasi

(Santosh Pandey)

CONTENTS

Title of Thesis	i
Certificate	ii
Declaration by the Candidate & Certificate by the Supervisor	iii
Copyright Transfer Certificate	iv
Dedication	v
Acknowledgement	vi-vii
Contents	viii-xiii
List of Figures	xiv- xviii
List of Tables	xix
List of symbols/ Abbreviation	xx-xxi
Preface	xxii-xxvi
CHAPTER – 1	1-52
Introduction of Perovskite	1
1.2. Perovskite substitution	3
1.2.1. Isovalent substitution	4
1.2.2. Heterovalent substitution	4
(a) Acceptors substitutions	4
(b) Donors substitutions	4
1.2.3. Valence compensated substitution	5
1.3. ABO ₃ type high dielectric constant Perovskites	5
1.3.1. CaTiO ₃	5
(a) Applications	7
1.3.2. Barium Titanate (BaTiO ₃)	7
1.3.3. SrTiO ₃	10
1.4. Complex Perovskite	13

CONTENTS

1.4.1. $\text{CaCu}_3\text{Ti}_4\text{O}_{12}$ (CCTO)	13
1.4.2. $\text{Y}_{2/3}\text{Cu}_3\text{Ti}_4\text{O}_{12}$ (YCTO)	15
1.4.3. $\text{Bi}_{2/3}\text{Cu}_3\text{Ti}_4\text{O}_{12}$ (BCTO)	16
1.5. Application of Perovskite	18
1.6. Composite Materials	17
1.6.1. Natural composites	17
1.6.2. Early composites	17
1.6.3. Making composites	18
1.6.4. Nanocomposite	19
1.6.5. Ceramic matrices Nanocomposite	21
1.6.6. Application of composites	22
1.7. Ceramic Dielectrics	22
1.7.1. Dielectric Behaviour	23
(a) Basic concept of dielectric capacitor	24
1.8. Polarization	26
1.8.1. Types of polarization:	26
(a) Electronic polarization:	26
(b) Ionic polarization:	26
(c) Dipolar polarization:	26
(d) Space charge polarization:	27
1.9. Dielectric constant	28
1.10. Dielectric loss	28
1.11. Basic Principles of Impedance Spectroscopy	31
1.12. Conductivity	34

CONTENTS

1.13. Magnetic Properties	34
1.13.1. Magnetism	36
(a) Electron magnetic moment	37
(b) Spin magnetic moments	37
1.13.2. Diamagnetic	38
1.13.3. Paramagnetic	39
1.13.4. Ferromagnetism	40
1.13.5. Magnetic Domain	40
1.13.6. Ant ferromagnetism	41
1.13.7. Ferrimagnetism	41
1.13.8. Superparamagnetism	42
(a) Applications	42
1.14. Aim of study	43
References	46
CHAPTER – 2	53-67
2.1. Experimental	53
2.2. Material used	54
2.2.1 Chemicals	54
2.3. Preparation of materials	55
2.3.1. Preparation of metal nitrate solution	55
2.4. Synthesis methods	55
2.4.1. Semi wet route	55
2.4.2. Solid State Route	57
2.4.2. Calcination Process	57
2.4.3 Sintering Process	57

CONTENTS

2.5. Characterization techniques for synthesized ceramic materials:	58
2.5.1. Phase and Crystal Structure Analysis:	58
2.5.3. Scanning Electron Microscopy (SEM) Analysis	60
2.5.4. Energy Dispersive X-ray Analysis (EDX)	61
2.5.5. Transmission Electron Microscopy (TEM) Analysis	62
2.5.6. Atomic force microscopy (AFM)	63
2.5.7. Superconducting quantum interference device (SQUID)	64
2.5.8. Electric and Dielectric Measurement:	65
2.5.9. Impedance and Conductivity	67
CHAPTER – 3	68-85
3.1. Introduction	68
3.2. Experimental	69
3.2.1. Synthesis	69
3.2.2. Characterization	70
3.3. Results and discussion	71
3.3.1. X-ray diffraction studies	71
3.3.2. Microstructural studies	72
3.3.3. Dielectric studies	75
3.3.4. Magnetic studies	78
3.4. Conclusion	81
References	82
CHAPTER – 4	86-102
4.1. Introduction	86
4.2. Experimental	88
4.2.1. Synthesis	88

CONTENTS

4.2.2. Characterization	89
4.3. Results and Discussion	89
4.3.1. X-ray diffraction studies	89
4.3.2. Microstructural studies	91
4.3.3. Dielectric Studies	95
4.4. Conclusion	98
References	99
CHAPTER – 5	103-120
5.1. Introduction	103
5.2. Experimental	104
5.2.1. Synthesis	104
5.2.2. Characterization	105
5.3. Results and Discussion	106
5.3.1. X-ray diffraction studies	106
5.3.2. Microstructural studies	107
5.3.3. Magnetic studies	111
5.3.4. Dielectric studies	114
5.4. Conclusion	117
References	118
CHAPTER – 6	121-135
6.1. Introduction	121
6.2. Experimental	123
6.2.1. Synthesis of materials	123
6.2.2. Structural and microstructural characterization	124
6.3. Result and Discussions	124

CONTENTS

6.3.1. X-ray diffraction studies	124
6.3.2. Microstructural studies	125
6.3.3. Dielectric studies	129
6.4. Conclusion	130
References	132
Summary and future scope	136-138
List of publications	139

Figure 1.1 A perovskite unit cell that displays the titanium ion off-centered.	6
Figure 1.2 Schematic of the perovskite structure of BaTiO ₃ (A) Cubic lattice (above Curie temperature, 120°C)	
(B) Tetragonal lattice (below Curie temperature, 120°C)	8
Figure 1.3. Reversal toward spontaneous polarization in BaTiO ₃ by reversal of the applied field direction.	9
Figure 1.4. Atomic structure of SrTiO ₃ at Room Temperature.	12
Figure 1.5. Atomic arrangements for the <100>, <110> and <111> axial direction in SrTiO ₃ .	12
Figure 1.6 Crystal structure of CCTO compound.	14
Figure 1.7. Crystal structure of BCTO, in which 1/3Bi sites are vacant. The Ti atoms sit at the center of the TiO ₆ Octahedra.	17
Figure 1.8. A polarized dielectric material.	23
Figure 1.9. Typical response of the total polarizability of a crystal as a function of electric field Frequency.	27
Figure 1.10. Types of polarization mechanisms	28
Figure 1.11. Simulated IS data for two RC elements connected in series, presented in different formats: Z'' [Ω] vs. frequency (f), M'' vs. f, Z'' [Ω] vs. Z' [Ω] and C' [Farad] vs. f.	33
Figure 1.12. Types of Magnetism.	36
Figure 1.13. Flow chart of Magnetism.	38
Figure 1.14. Ferromagnetic and super paramagnetic.	42
Figure 2.1. Flow chart for the synthesis of materials by semi-wet route	54

Figure 2.2. Powder XRD instrument, RigakuMiniflex600 (Japan)	59
Figure 2.3 Braggs law of diffraction	59
Figure 2.4 Scanning Electron microscopy (SEM, ZEISS model, EVO-18 Germany) and EDX Analysis instrument (Oxford instrument; USA)	62
Figure 2.5 Transmission electron microscope (TEM, FEI Tecnai-20G2) used for determination of particle structure.	63
Figure 2.6 Superconducting quantum interference device (SQUID) (Quantum Design, MPMS 3)	65
Figure 2.7 LCR Meter (PSM 1735, Newton 4th Ltd, U.K.) used for dielectric measurement.	67
Figure 3.1 XRD diffraction pattern of sintered CCTMO at 1223K for 8 h.	72
Figure 3.2 (a) Bright field TEM images (b) Selected area diffraction pattern (SEAD) of CCTMO ceramics sintered at 1223K at 8h.	73
Figure 3.3 SEM images of CCTMO ceramics sintered at 1223K for 8h, (a) SEM images of CCTMO (b) EDX spectra of CCTMO ceramic.	74
Figure 3.4 AFM images of CCTMO ceramics sintered at 1223 K for 8 h, (a) 2-dimensional structure (b) 3-dimenional structure (c) bar diagram of particle size.	75
Figure 3.5 Temperature dependent (a) dielectric constant (ϵ_r), and (b) dielectric loss ($\tan \delta$) at few selected frequencies.	77
Figure 3.6 Frequency dependent (a) dielectric constant (ϵ_r) and (b) Dielectric loss ($\tan \delta$) at few selected Temperature.	77

Figure 3.7 Temperature dependent (a) magnetic moment noted at ± 2 T and magnetic field at 100 Oe. (b) M-H hysteresis at 5 and 300 K for CCTMO ceramic. 79

Figure 3.8 Magnetic susceptibility as a function of temperature recorded at ± 2 T and applied magnetic field (H) at 100 Oe. 80

Figure 3.9 P-E hysteresis loop for $\text{CaCu}_3\text{TiMnO}_{12}$ sintered at 1223 K for 8 h. 81

Figure 4.1 XRD patterns of $\text{CaCu}_3\text{Ti}_{4-x}\text{Mn}_x\text{O}_{12}$ (a) $x= 0.25$ (b) $x= 0.50$ (c) $x= 1.00$ sintered at 1223 K for 8 h. 90

Figure 4.2 Bright field TEM images and their corresponding SEAD patterns of sintered $\text{CaCu}_3\text{Ti}_{4-x}\text{Mn}_x\text{O}_{12}$ ceramic (0.25, 0.50 and 1.00). 92

Figure 4.3 SEM micrograph of $\text{CaCu}_3\text{Ti}_{4-x}\text{Mn}_x\text{O}_{12}$ ceramics (a) $x= 0.25$ (b) $x= 0.50$ (c) $x= 1.00$ and EDX spectra of $\text{CaCu}_3\text{Ti}_{4-x}\text{Mn}_x\text{O}_{12}$ ceramics (d) $x= 0.25$ (e) $x=0.50$ (f) $x=1.00$ sintered at 1223 K for 8 h. 93

Figure 4.4 AFM images of $\text{CaCu}_3\text{Ti}_{4-x}\text{Mn}_x\text{O}_{12}$ ($x=1.00$) ceramics sintered at 1223 K for 8 h (a) 2-dimentional structure (b) 3-dimentional structure (c) bar diagram of particle size. 94

Figure 4.5 Dielectric constant (ϵ_r) as the function of frequency for $\text{CaCu}_3\text{Ti}_{4-x}\text{Mn}_x\text{O}_{12}$ ceramics ($x=0.25, 0.50$ and 1.00) sintered at 1223 K for 8 h. 96

Figure 4.6 Dielectric loss ($\tan \delta$) as the function frequency $\text{CaCu}_3\text{Ti}_{4-x}\text{Mn}_x\text{O}_{12}$ ceramics ($x=0.25, 50$ and 1.00) sintered at 1223 K for 8 h. 96

Figure 4.7 P-E hysteresis loop for $\text{CaCu}_3\text{Ti}_{4-x}\text{Mn}_x\text{O}_{12}$ ceramics ($x= 0.25, 0.50$ and 1.00) at room temperature. 97

Figure 5.1 XRD patterns of CCTMO sintered at (a) 1223 K (b) 1323 K (c) 1373 K for 8 h. 106

- Figure 5.2** Bright-field TEM images at (a) 1223 K (b) 1323 K (c) 1373 K and (d) Selected area diffraction pattern of CCTMO at 1373 K. 108
- Figure 5.3** (a-c) SEM micrograph and (d-e) EDX spectra of CCTMO ceramic sintered at 1223 K, 1323 K, and 1373 K, respectively for 8 h. 110
- Figure 5.4** AFM images of CCTMO ceramics sintered at 1373 K for 8 hours (a) 2-dimensional structure (b) 3-dimensional structure (c) bar diagram of particle size. 112
- Figure 5.5** Temperature-dependent (a) magnetic moment noted applied magnetic field at 100 Oe. (b) M-H hysteresis at 5 and 300 K for CCTMO ceramic sintered at 1323 K for 8 h. 112
- Figure 5.6** Magnetic susceptibility as a function of temperature recorded at ± 2 T and applied magnetic field (H) at 100 Oe. 113
- Figure 5.7** The polarization versus electric field (P-E) hysteresis loop of $\text{CaCu}_3\text{Ti}_{3.5}\text{Mn}_{0.5}\text{O}_{12}$ at sintered at 1223 K, 1323 K, and 1373 K, respectively. 114
- Figure 5.8** Temperature-dependent (a) dielectric constant (ϵ_r) and (b) loss tangent ($\tan \delta$) at 10 kHz for sintered at 1223 K, 1323 K, and 1373 K, respectively for 8 h. 116
- Figure 5.9** Frequency-dependent (a) dielectric constant (ϵ_r) and (b) loss tangent ($\tan \delta$) at room temperature for sintered at 1223 K, 1323 K, and 1373 K, respectively. 117
- Figure 6.1** XRD patterns of $\text{CaCu}_3\text{Ti}_{3.5}\text{X}_{0.5}\text{O}_{12}$ (a) X= Mn (b) X= Nb (c) X= W sintered at at 1223 K, 1323 K and 1373 K, respectively for 8 h. 125

Figure 6.2 Bright-field TEM images and their corresponding SEAD patterns of $\text{CaCu}_3\text{Ti}_{3.5}\text{X}_{0.5}\text{O}_{12}$ ceramics (a-b) X= Mn (c-d) X= Nb (e-f) X= W (Mn, Nb and W) sintered at 1223 K, 1323 K and 1373 K, respectively for 8 h. 126

Figure 6.3 SEM micrograph of $\text{CaCu}_3\text{Ti}_{3.5}\text{X}_{0.5}\text{O}_{12}$ ceramics (a) X= Mn (b) X= Nb (c) X= W and EDX spectra of $\text{CaCu}_3\text{Ti}_{3.5}\text{X}_{0.5}\text{O}_{12}$ ceramics (d) X= Mn (e) X= Nb (f) X= W sintered at 1223 K 1323 K and 1373 K, respectively for 8 h. 127

Figure 6.4 X-ray photo emission spectroscopy (a) Mn 2p, (b) Nb 3d, (c) W 4f, for CCTXO (X= Mn, Nb, W) sintered at 1223 K, 1323 K and 1373 K, respectively for 8 h. 128

Figure 6.5(a). Dielectric constant (b) dielectric loss dependent on the frequency at a few selected temperatures of CCTMO sintered at 1223 K for 8h. 130

Figure 6.6(a). Dielectric constant (b) dielectric loss dependent on the frequency at a few selected temperatures of CCTNO sintered at 1323 K for 8h. 130

Figure 6.7(a). Dielectric constant (b) dielectric loss dependent of frequency at a few selected temperatures of CCTWO sintered at 1373 K for 8h. 130

TABLES

Table 1.1: Summary of the physical properties of SrTiO ₃ .	11
Table 2.1 Specification of the chemical used.	54
Table 4.1 Atomic percentage of elements for CaCu ₃ Ti _(4-x) Mn _x O ₁₂ ceramics (x= 0.25, 0.50 and 1.00) sintered at 1223 K for 8 h.	93
Table 5.1 Atomic percentage of elements for CaCu ₃ Ti _{3.5} Mn _{0.5} O ₁₂ sintered at 1223 K, 1323 K and 1373 K, respectively for 8 h.	109

E	Permittivity or dielectric constant
ϵ^*	Complex Quantity of dielectric constant
ϵ'	real components of dielectric constant
ϵ''	Imaginary component of dielectric constant
i	Imaginary number
ϵ_0	Permittivity of free space
ϵ_r	relative dielectric constant
C	Capacitance
F	Farad
$\tan \delta$	tangent loss
σ	conductivity
f	frequency
λ	Wavelength
θ	Angle theta
$^{\circ}\text{C}$	Degree centigrade
K	Kelvin
k_B	Boltzmann constant
T_B	Blocking temperature
χ	Magnetic susceptibility
C	Curie constant
M	Magnetization
H	Magnetic field
Oe	Oersted
P	Density
B	Induced magnetic field
E	Electric field

P	Net polarization
P _{electronic}	Electronic polarization
P _{ionic}	Ionic polarization
P _{molecular}	Molecular polarization
P _{interfacial}	Interfacial polarization
Hz	hertz
ω	angular frequency
τ	Relaxation time
t	tolerance factor
Å	angstrom
R	Resistance
C	Capacitance
R _b	Resistance of bulk
C _b	Capacitance of bulk
R _{gb}	Resistance of grain boundary
C _{gb}	Capacitance of grain boundary
eV	electron Volt

PREFACE

A capacitor material which has high dielectric constant and low dielectric loss is an interesting topic in materials science. It may be used as multilayer capacitor (MLCC), dynamic random access memory (DRAMs), microwave devices, electronic devices in automobiles and aircrafts. $ACu_3Ti_4O_{12}$ ($A = Ca, Bi, Sr$) type oxides had complex perovskite structure and discovered in 1967 by Subramanian *et al.* It produces a high dielectric constant ($\epsilon_r \sim 10^4$) and nearly constant in the temperature range of 100–600 K. which has led to many important applications. The high dielectric loss of CCTO ceramics ($\tan \delta > 0.05$ at 1 kHz) is still the most serious problem for applications requiring capacitive components. Presently we use simple perovskite $BaTiO_3$, which are not environmentally friendly as capacitor materials. The problem with $BaTiO_3$ is that it is quite unstable at higher and shows phase transition. Therefore, it is not suitable for use at high temperature. Therefore, Development of excellent dielectric materials with good stability over wide temperature and frequency ranges are highly desired.

The modern age technology needs for the development of electrical composite, that properties are not available in individual single component materials. The required combination properties are possible to tailor composite by combining two or more components. Composites perovskite play a very important role in various areas of chemistry, physics, biology and materials science because of their interesting properties. When two or more perovskites are mixed together either by physical or by chemical methods to fabricate composite, a novel set of physical and chemical properties may be obtained that would be completely different from that of the individual constituents.

Electrical and dielectric properties of the composite are also very important. Which leads to data storage, tunnel junction, and spin valves. The composite has also been increasing interest in flexible, high dielectric constant and a polymer for use in

PREFACE

high-density energy storage and capacitor applications. With the smaller sizes of nanoparticle less than 100 nm surfaces to volume ratio increases resulting in the number of atoms on the surface of nanocrystals, therefore variation in electrical properties with change in structure in the nanoscale region is observed in comparison to the bulk material. The electrical and dielectric properties of nanoparticle are affected by particle size, morphology, and chemical composition.

In the present work synthesis of composite perovskite with different composition using semi-wet route. All the synthesized composites were characterized by various physicochemical techniques to study the crystal structure, particle size and shape whereas electrical and dielectric, properties of materials were studied in detail. And it also studied the effect of sintering duration of these composite.

The present work aims to investigate (a) crystal structure (b) microstructure (c) elemental analysis (d) particle size (e) electrical and dielectric behavior of the following compound prepared by semi-wet route.

1. $\text{CaCu}_3\text{Ti}_3\text{MnO}_{12}$
2. $\text{CaCu}_3\text{Ti}_{3.5}\text{Mn}_{0.5}\text{O}_{12}$
3. $\text{CaCu}_3\text{Ti}_{3.75}\text{Mn}_{0.25}\text{O}_{12}$
4. $\text{CaCu}_3\text{Ti}_{3.5}\text{W}_{0.5}\text{O}_{12}$
5. $\text{CaCu}_3\text{Ti}_{3.5}\text{Nb}_{0.5}\text{O}_{12}$

Chapter I This chapter contains a brief introduction of the subject describing briefly the technical investigations reported in the field of perovskite oxides and composite materials. Polarization also describes which related to dielectric properties as well as the

PREFACE

frequency of perovskite. It contains basic knowledge of Impedance spectroscopy which separates the contributions of the grains and grain boundaries, and electrode specimen interface observed RC elements of the composite. This includes the effect of isovalent, heterovalent and valence compensated substitutions on the electrical and dielectric properties.

Chapter II This chapter describes the details of experimental procedure used for the synthesis, characterization, and application of composite materials. The crystalline phases of composite sintered samples were identified by using the X-ray diffraction analysis (Rigaku, miniflex-600, Japan) employing Cu- α radiation. Scanning Electron Microscopy gives an idea of formation of the microstructure of these materials. Transmission Electron Microscopy (TEM) has been used for determination of their size and shape of the particle. Atomic force microscopy analyzed the surface morphology. Electrical and dielectric properties which are characteristic of all the composite were measured as a function of temperature (300-500 K) in the frequency range 100Hz-5 MHz with the help of PSM 1735 (NumetriQ 4th U.K Limited) LCR Meter.

Chapter III The detailed synthesis, characterization and application of the $\text{CaCu}_3\text{Ti}_4\text{MnO}_{12}$ (CCTMO) perovskite were described in this chapter. CCTMO was synthesized using a semi-wet method through sintering at 1223 K for 8 h. The structural and microstructural details were studied by X-ray diffraction (XRD), scanning electron microscope (SEM) and transmission electron microscope (TEM) techniques. XRD analysis confirmed the existence of $\text{CaCu}_3\text{Ti}_4\text{O}_{12}$ (CCTO) as the primary phases along with TiO_2 as the minor aspects. The average grain sizes obtained by SEM analysis were found to be around 1.46 μm sintering for 8 h, respectively. TEM analysis showed the particle size in the range of 43.76 ± 10 nm. The surface morphology was analyzed by

PREFACE

atomic force microscopy (AFM). The sample sintered for 8 h exhibited very high dielectric constant ($\epsilon_r \sim 100$) at 1 kHz and 303 K. The presence of semiconducting grains with the insulating grain boundaries significantly attributes to such a high dielectric constant value, supporting the internal barrier layer capacitance (IBLC) mechanism operative in CCTMO perovskite.

Chapter IV In this chapter, the $\text{CaCu}_3\text{Ti}_{(4-x)}\text{Mn}_x\text{O}_{12}$ (CCTMO) was synthesized by a semi-wet method at 1223 K for 8 h. X-ray diffraction (XRD) analysis confirms the presence of CCTMO and $\text{CaCu}_3\text{Ti}_4\text{O}_{12}$ both phases in the perovskite ceramic. Transmission electron microscope (TEM) analysis of the composite demonstrates the formation of nanoparticles with average particle size 23 ± 10 nm, 31 ± 10 nm and 24 ± 10 nm at a different doping concentration of Mn ($x= 0.25, 0.50$ and 1.00) in $\text{CaCu}_3\text{Ti}_{4-x}\text{Mn}_x\text{O}_{12}$ ceramic.. The surface morphology of the composite sintered at 1223 K for 8 h obtained by SEM analysis indicate the formation of large and small grains with bimodal structure. The average and root mean square roughness is found to be 72 nm and 90 nm, respectively by Atomic force microscopy studies of the ceramic. The dielectric constant of CCTMO ceramic is found to be 150 at 100 Hz and 500 K respectively. The presence of semiconducting grains and insulating grain boundaries in the composite supporting the internal barrier layer capacitance (IBLC) mechanism operative in Mn-doped CCTO type of perovskites of different composition.

Chapter V The synthesis, characterization and application of the $\text{CaCu}_3\text{Ti}_{3.5}\text{Mn}_{0.5}\text{O}_{12}$ ceramic were discussed in this chapter. A nano-composite ceramic with the chemical composition $\text{CaCu}_3\text{Ti}_{3.5}\text{Mn}_{0.5}\text{O}_{12}$ was synthesized by a semi-wet method at CCTMO sintered at 950 °C, 1050 °C, and 1100 °C, respectively for 8 h. X-ray diffraction analysis confirms the presence of CCTO and TiO_2 phases in the composite ceramic.

PREFACE

Transmission electron microscope analysis of the formation of nano-particles (98.49 ± 10 nm, 92.95 ± 10 nm and 145.50 ± 10 nm at 950 °C, 1050 °C, and 1100 °C, respectively). Further, scanning electron microscope (SEM) images show that the morphology consists of large and small grains ($1.0\text{--}10$ μm) with a bimodal distribution. The surface morphology of composite was studied by atomic force microscope using tapping mode of measurement also substantiates the results obtained by SEM analysis. The sample sintered for 8 h exhibits very high dielectric constant ($\epsilon_r \approx 130$) at 100 Hz and room temperature. The presence of semiconducting grains with insulating grain boundaries significantly attributes to such a high dielectric constant value, supporting the internal barrier layer capacitance mechanism operative in Mn-doped CCTO of different composition.

Chapter VI the CCTMO, CCTWO and CCTNO perovskites were successfully synthesized by semi-wet route. Powder X-Ray Diffraction confirms the formation of CCTO as main phase along with minor TiO_2 phase in CCTMO, CCTWO and CCTNO at sintered at 950°C , 1050°C , and 1100°C , for 8 h. Particle size observed by TEM is 44 nm, 101 nm, and 51 nm, respectively. Atomic force microscopy shows statistically significant changes in the surface roughness. The nano-composite exhibits improvement in dielectric loss ($\tan \delta \approx 0.9$) at 1 kHz. The low-frequency performance of the doped CCTO was estimated by measuring the frequency dispersion of the dielectric constant (ϵ') and dielectric loss ($\tan \delta$).